Piezoelectric charge densities in AlGaN/GaN HFETs

P.M. Asbeck, E.T. Yu, S.S. Lau, G.J. Sullivan, J. Van Hove and J. Redwing

Indexing terms: Microwave power transistors, Gallium nitride, Field effect transistors

New estimates of the piezoelectric charge density at (0001) AlGaN/GaN interfaces are provided. Undoped HFET structures grown by both MBE and MOCVD, on sapphire and SiC substrates, exhibit electron densities of $\sim 5 \times 10^{13}$ cm$^{-2} \cdot x_{Al}$ (where x_{Al} is the aluminium mol fraction in the AlGaN), which can be attributed to piezoelectric effects. These have a significant influence on the design and behaviour of III-V nitride HFETs.

Introduction: Heterostructure field-effect transistors (HFETs) based on the AlGaN/GaN system have recently been shown to be very attractive candidates for high voltage, high power amplification at frequencies well into the microwave region [1 – 4]. The behaviour of these devices is under intense investigation. It has previously been shown that the nitrides have appreciable piezoelectric coefficients, and that on (0001) faces of the wurtzite structures typically used to form HFETs, electric polarisation should occur, resulting in potentially large charge densities and associated electric fields [5, 6]. In this Letter, we report new estimates of the magnitude of these charge densities and detail a number of their expected effects on HFET characteristics.

Analysis: A representative FET layer structure consists of a 50nm layer of AlGaN, on top of a 3μm layer of GaN, deposited on a substrate of sapphire or SiC. Appreciable 2D electron gas (2-DEG) densities are found at the AlGaN/GaN interface, even if all the layers are grown without intentional doping [7]. The layers are usually under stress due to either a lattice mismatch between epitaxial layers of different alloy compositions, or a thermal expansion mismatch between the epitaxial layers and the substrate (which may be partially or entirely relaxed). There is, in particular, a large amount of strain at the AlGaN/GaN interface, due to the difference in lattice constants between these two materials (2.4% difference between AlN and GaN at room temperature). The biaxial stress and strain associated with the lattice mismatches generates a piezoelectric polarisation P_z (where the z axis lies along the [0001] direction, normal to the HFET surface), given by [5]

$$P_z = 2d_{31}(c_{11} + c_{12} - 2c_{13}^2/c_{33})\varepsilon_{xx} \qquad (1)$$

Here, d_{31} is the piezoelectric strain ceofficient for AlGaN, c_{ij} are the elastic stiffness coefficients, and ε_{xx} is the strain in the x direction (taken to be equal to ε_{yy}. The electrical effects of the polarisation can be determined by considering that there is a piezoelectrically-induced charge density $Q_{pz} = qN_{pz} = div\mathbf{P}$. At the interface between pseudomorphically-grown AlGaN and GaN, there is a change in strain (and stress) because of the difference in lattice-constants. Correspondingly, there is a piezoelectric positive (donor-like) charge density due to the difference between the polarisations within the AlGaN and the GaN. The magnitude of the interfacial charge density is essentially independent of the level of strain common to both AlGaN and GaN (assuming equal piezoelectric coefficients for the two materials), and thus is independent of the details of the substrate, buffer and sample bending. At the top of the AlGaN layer (and, possibly, at the bottom of the GaN layer) there will be negative (acceptor-like) PZ charge densities. The PZ charge density at the AlGaN/GaN interface will be largely compensated for by electrons that form a 2D electron gas at the interface; charge at the top of the AlGaN will be compensated for by either charged surface states for a free surface, or carriers in the metal layer for a metal contact. A schematic, approximate, band diagram of the resulting undoped AlGaN/GaN interface is shown in Fig. 1, along with a schematic representation of the charge densities.

The sign of the piezoelectric charges is dependent on the crystal orientation. GaN and AlGaN layers grown by MBE and MOCVD typically grow in (0001) directions, that is, with the A (or Ga) face at the surface [8]. According to eqn. 1, and the value of $d_{31} = -2 \times 10^{-10}$cm/V for AlN given in [9], donor-like PZ charges result at the AlGaN/GaN interfaces (although this assignment differs from [5, 6]). Polarisation is directed from the A face to the B face (as is the case in CdS, which also forms in the wurtzite structure and has $d_{31} < 0$ [9]). For crystals grown on (000_1) or B faces, an opposite sign of charge is expected.

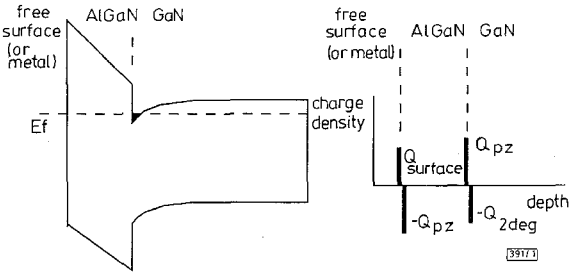

Fig. 1 *Band diagram and schematic doping density resulting from piezoelectric charge density*

The density of electrons in the 2-DEG at the interface departs somewhat from the piezoelectrically-induced (PZ) donor density N_{pz}, because a net charge density is required to terminate the electric field in the AlGaN layer. This electric field is fixed by the potential drop in the AlGaN determined by the fermi level positions at the surface and at the interface. We find that the 2-DEG density is given by

$$N_s = N_{pz} - C_b(\phi_s - \Delta E_c + \varepsilon_{fn}(N_s))/q \qquad (2)$$

Here, N_{pz}, the PZ donor density at the interface, is given by $N_{pz} = (P_{1z} - P_{2z})/q$. C_b is the geometric capacitance associated with the AlGaN layer of thickness h_b ($C_b = \varepsilon/h_b$); ϕ_s is the depth of the fermi level at the AlGaN surface with respect to its conduction band edge, ΔE_c is the conduction band offset between AlGaN and GaN (in the given strained condition), and ε_{fn} is the height of the fermi level above the conduction band in the GaN (which is a function of N_s). P_{1z} and P_{2z} are the polarisations in the AlGaN and the GaN, associated with the strains ε_{xx1} and ε_{xx2} in the two materials, respectively. Assuming a coherent interface between the layers, by Vegards law, we expect $\varepsilon_{xx1} - \varepsilon_{xx2}$ is proportional to the aluminium mol fraction of the AlGaN layer. Thus, N_{pz} is approximately proportional to x_{Al}. In general, however, d_{31} may vary with x_{Al} (and probably increases in magnitude as the aluminium content rises).

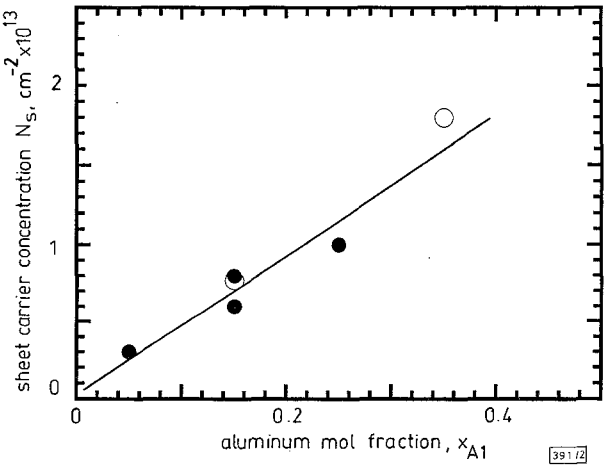

Fig. 2 *Experimental values of N_s against x_{Al} for various undoped MBE- and MOCVD-grown AlGaN/GaN HFET structures*

● MOCVD grown
○ MBE grown

Experimental results: In Fig. 2 the measured sheet carrier concentrations N_s are shown against x_{Al} in AlGaN/GaN HFET structures grown without intentional doping. These data were obtained from Hall measurements on structures with free surfaces. The data include reported values for MOCVD [7], as well as for MBE growth (shown here for the first time). The results of the two growth methods agree well, and indicate a value of N_s that rises approximately linearly with x_{Al}, following $dN_s/dx_{Al} = 5 \times 10^{13}$cm^{-2}. This slope may rise slightly for increasing x_{Al}. The results for both sapphire substrates and SiC coincide closely.

Discussion: The origin of the charges in these undoped FETs has not yet been identified [7]. The assignment of the observed charge densities to the 'piezoelectric doping' described here is more plausible than assuming that there are residual impurities in the GaN or AlGaN. It has been reported that samples of GaN or AlGaN grown individually have resulted in low doping levels. Also, Fig. 2 shows the essential equivalence of MBE and MOCVD-grown materials, which may be expected to have different residual doping levels.

In accordance with eqn. 2, the electron density at the interface for a given value of x_{Al} is expected to vary somewhat as a function of thickness of the AlGaN layer, and the overall value of N_s is expected to be lower than N_{pz} The data suggest that the difference $N_{pz} - N_s$ is relatively small. This may correspond to the fact that the electric field in the AlGaN layer is small.

The experimental value of dN_s/dx_{Al} obtained by fitting the data of Fig. 2 is larger, by a factor of 1.8, than the corresponding value estimated by Martin *et al.* based on published values of piezoelectric coefficients [6]. To make the earlier estimates, an interpolation had been necessary in order to arrive at an estimate for d_{31} of GaN. The bowing of the curve of N_s against x_{Al} suggests that d_{31} increases with x_{Al}.

The dominance of PZ charge densities has numerous consequences for the HFET design. Although the PZ charge exists at the plane of the heterojunction, it is not expected to degrade the mobility of the 2-DEG, because the PZ charge is very uniformly distributed (with every atom at the heterojunction having a small amount of strain-induced charge) unless substantial interface roughness is present. Recessing the Schottky gate region produces only a minor effect on the threshold voltage (since N_s varies only slowly with h_b). Reducing the AlGaN thickness in the source and drain ohmic contact regions can assist in producing ohmic contacts, but etching it away completely can eliminate the conductivity in the underlying GaN. Also, buffer layers of AlGaN beneath a thin conducting channel produce distortions of carrier densities in the channel, due to the PZ charges at their interfaces. The extremely strong influence of PZ effects on device behaviour suggests numerous additional possibilities for design and optimisation of III-V nitride devices.

Conclusion: We have shown that, through the PZ effect, donor-like charge densities of the order of $5 \times 10^{13}\text{cm}^{-2} \cdot x_{Al}$ are produced at pseudomorphic AlGaN/GaN interfaces. The existence of the piezoelectric charges provides an insight into the relative performances of various HFET structures.

Acknowledgments: The authors are grateful to B. McDermott, R. Pierson, E. Gertner, M.F. Chang, T. Kuech, and Q.Z. Liu for helpful conversations. Financial support from BMDO (Kepi Wu), monitored by US Army SSDC, is gratefully acknowledged.

21 May 1997
Electronics Letters Online No: 19970843

P.M. Asbeck, E.T. Yu and S.S. Lau (*Department of Electrical and Computer Engineering, University of California, San Diego, La Jolla, CA 92093-0407, USA*)

G.J. Sullivan (*Rockwell Science Center, Thousand Oaks, CA, USA*)

J. Van Hove (*SVT Associates, Eden Prairie, MN, USA*)

J. Redwing (*Advanced Technology Materials, Inc., Danbury, CT, USA*)

References

1 KHAN, A., CHEN, Q., SHUR, M.S., MCDERMOTT, B.T., HIGGINS, J.A., BURM, J., SCHAFF, W., and EASTMAN, L.F.: 'Short-channel GaN/AlGaN doped channel heterostucture FETS with 36GHZ cutoff frequency', *Electron. Lett.*, 1996, **32**, p. 357

2 AKTAS, O., KIM, W., FAN, Z., STENGEL, F., BOTCHKAREV, A., SALVADOR, A., SVERLOV, B., MOHAMMAD, S.N., and MORKOC, H.: 'High transconductance GaN MODFETs'. Tech. Dig. 1995 IEDM, 1995, p. 205

3 WU, Y.F., KELLER, B.P., KAPOLNEK, D., KOZODOY, P., DENBAARS, S.P., and MISHRA, U.K.: 'Very high breakdown voltage and large transconductance realised on GaN heterojunction FETs', *Appl. Phys. Lett.*, 1996, **69**, p. 1438

4 BINARI, S.C., REDWING, J.M., KELNER, G., and KRUPPA, W.: 'AlGaN/GaN HEMTs grown on SiC substrates', *Electron. Lett.*, 1997, **33**, p. 242

5 BYKHOVSKI, A., GELMONT, B., and SHUR, M.: 'The influence of the strain-induced electric field on the charge distribution in GaN-AlN-GaN structure', *J. Appl. Phys.*, 1993, **74**, p. 6734

6 MARTIN, G., BOTCHKAREV, A., ROCKETT, A., and MORKOC, H.: 'Valence-band discontinuities of wurtzite GaN, AlN, and InN heterojunctions measured by x-ray photoemission spectroscopy', *Appl. Phys. Lett.*, 1996, **68**, p. 2541

7 REDWING, J.M., FLYNN, J.S., TISCHLER, M.A., MITCHEL, W., and SAXLER, A.: 'MOVPE growth of high electron mobility AlGaN/GaN heterostructures'. Proc. Mat. Res. Soc. Symp., 1996, p. 395

8 PONCE, F.A., BOUR, D.P., YOUNG, W.T., SAUNDERS, M., and STEEDS, J.W.: 'Determination of lattice polarity for growth of GaN bulk single crystals and epitaxial layers', *Appl. Phys. Lett.*, 1996, **69**, p. 337

9 LANDOLT-BORNSTEIN: 'Numerical data and functional relationships in science and technology' (Springer, New York, 1982)

1.8Petabit/s downstream capacity WDM passive optical network

C.R. Giles, C. Doerr, M. Zirngibl, C. Joyner, U. Koren, K.F. Dryer, J. Zyskind, J. Sulhoff, L. Stulz and C. Wolf

Indexing terms: Passive networks, Optical communication, Wavelength division multiplexing

The ability to provide a 55Mbit/s service to 33.5million PON subscribers is described, using an 8-channel sequentially-pulsed 1555nm integrated multifrequency laser distributed to 4.3million WDM PON lines through five amplifier/splitter stages. The wavelength-encoded pulses were modulated at 440Mbit/s with an InGaAsP electroabsorption modulator, and then, after 20km transmission through singlemode fibre, they were demultiplexed with an arrayed-waveguide grating router. Error-free transmission was achieved.

Introduction: While terabit/second data streams have been sent through point-to-point optical fibre connections [1 – 3], there has not been a demonstration of how to use this capacity in communication lines connected to a large number of local access subscribers. Passive optical networks are leading candidates for the future delivery of high-capacity (>50Mbit/s) bidirectional communication services between the central office and the subscriber premises. However, most wavelength-division multiplexed (WDM) architectures are not easily scaled to large numbers of customers because of the high cost of generating WDM channels. One proposed method is to distribute wavelength-encoded pulse streams from a centralised WDM source to a large number of PONs that terminate with synchronised optical modulators in the central office to generate subscriber data [4, 5]. The cost of the WDM PON is then moved from the WDM pulse source to the pulse distribution fabric and PON modulators, which may lead to improved cost models with a highly-shared fabric.

Here we describe the capability of distributing an 8-channel, sequentially-pulsed 1555nm WDM source to 4.3million, 20km length, PON lines through a five-stage amplifier/splitter cascade. The subscriber data rate was 55Mbit/s, yielding an aggregate network data rate of 1.8Pbit/s. This is different from large-scale broadcast distribution [6] as each subsciber in the access network now receives his own unique data channel. Such large-scale capacity in an access network leads to interesting speculation as to the number of tbit/s lines and switch sizes required to service such networks, and how a population might use an information density of $1.8 \times 10^{15}/\pi 20000^2 = 1.5$Mbit/s per square metre in a 20km radius. This density is equivalent to providing an OC-3 connection to every resident of New York City.

Results: The layout of the cascade-distributed sequentially-pulsed 1555nm WDM source and WDM PON is shown in Fig. 1. Eight channels of an integrated multifrequency laser [7] having 100GHz channel spacing were sequentially modulated at a channel rate of 55megapulses per second with an 8% pulse duty cycle. The pulses were interleaved 2.25ns apart, resulting in a 440megapulses per